(Received 30 October 2023, Accepted 15 January 2024, Scheduled 28 January 2024)

Sensorless Control of Permanent Magnet-Assisted Synchronous Reluctance Motor Based on Adaptive Sliding Mode Observer

Aide Xu[2,*], Xinyu Li[1], Shimai Hu[2], and Xin Liu[1]

[1] College of Marine Electrical and Engineering, Dalian Maritime University, Dalian 116026, China
[2] College of Information and Science Technology, Dalian Maritime University, Dalian 116026, China

ABSTRACT: To solve the issue of chattering that occurs during the estimation of the rotor position in the permanent magnet-assisted synchronous reluctance motor using the conventional sliding mode observer (SMO), the saturation function is used in this paper instead of the original sign function to reduce its jittering effect; to solve the problem of phase delay caused by the low-pass filter (LPF), the adaptive law is implemented as a substitute for the LPF. This allows for a smoother back electromotive force and eliminates the need for position compensation caused by phase delay; finally, the phase-locked-loop (PLL) technique is used to extract more accurate rotor position information. A 3 kW permanent magnet-assisted synchronous reluctance motor is taken as the control object, and a simulation model of the control system is established. The results show that the improved saturation function adaptive SMO has higher level of accuracy in estimating rotor position information than the conventional SMO.

1. INTRODUCTION

Permanent Magnet Assisted Synchronous Reluctance Motor (PMA-SynRM) was firstly proposed by Italian scholars Vagati et al. [1], and PMA-SynRM was not well developed due to the limitation of process and material level at that time. Due to the scarcity of rare earth resources, the PMA-SynRM, which has a low dependence on rare earths, a wide speed range, and high-power density, has once again become a research hotspot. It is widely used in fields such as electric vehicles, aerospace, and medical devices [2–4].

PMA-SynRM is a kind of motor that combines the advantages of permanent magnet synchronous motor (PMSM) and synchronous reluctance motor (SynRM), which has the features of lower cost, large pole-to-pole ratio, high power density, and easy control of demagnetization current [5–8]. In terms of control, PMA-SynRM is based on reluctance torque, supplemented by the permanent magnet torque, and often adopts the Maximum Torque per Ampere control method [9]. The vector control of the PMA-SynRM often adopts the installation of rotary transformers or photoelectric encoders on the shaft to obtain the rotor position information, which will increase the cost of production of the motor and reduce the reliability of the motor drive system [10]. Therefore, the position sensorless vector control of PMA-SynRM has become a research direction.

In recent years, the position sensorless control of PMA-SynRM has been widely studied by scholars. Studies have shown that different algorithms are often used in different speed domains: at zero and low speeds, the pulse signal injection method is usually used to obtain the position information of the rotor from the stator current because the motor generates a small back electromotive force, and the signal is not obvious [11]. At medium and high speeds, due to the more pronounced back electromotive force of the motor and magnetic chain, methods based on the fundamental wave model include the Extended Kalman Filter method, Model Reference Adaptive method, and Sliding Mode Observer (SMO) method, which are widely used. Among them, sliding mode works by bringing the dynamic state of the system to the sliding surface and then to the center point [12]. Sliding mode observer has the characteristics of insensitivity to parameters and good robustness, which is more suitable for permanent magnet-assisted synchronous reluctance motors with large convex pole ratio. Some scholars have directly applied the sliding mode observer technique and vector control strategy to the PMA-SynRM position sensorless speed control of a direct-drive washing machine, and the results show that it has a certain degree of engineering practicability [13], and the literature uses the sliding mode observer and high-frequency signal injection to carry out sensorless control of ferrite permanent magnet-assisted synchronous reluctance motors over a wide speed regulation range [14].

However, the inherent chattering problem of the conventional SMO and the phase compensation problem brought by the low-pass filter will increase the energy consumption and computational burden of the system and affect the estimation accuracy. In order to improve this problem, some scholars have used segmented exponential function to replace the sign function in the conventional sliding mode observer, which effectively weakens the chattering phenomenon of the conventional sliding mode observer; some scholars have also used the superhelix algorithm to design an improved sliding mode observer for the position sensorless control of the PMA-SynRM, and the

* Corresponding author: Aide Xu (aidexu@dlmu.edu.cn).

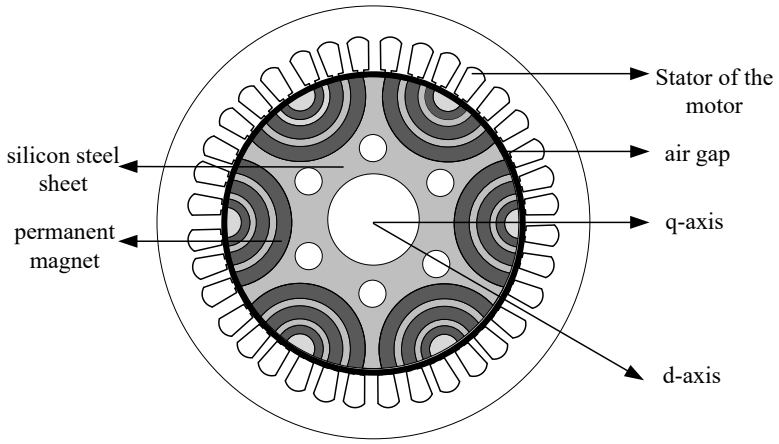

FIGURE 1. Schematic of the structure of PMA-SynRM.

results show that it has a good anti-chattering property and dynamic and static performance [15, 16]. However, the existence of Low-Pass Filter (LPF) makes the obtained back electromotive force still have high frequency harmonics, and in order to improve the problem, [17] designed a two-stage filtering structure combining a variable cutoff frequency low-pass filter and a modified back electromotive force observer in a sliding mode observer, which improves the adaptive capability of the low-pass filter in the case of high-frequency harmonic variations of the back electromotive force, but there is still a position compensation link in the process of rotor calculation.

In this paper, a new improvement strategy is proposed to solve the problem of chattering and phase delay caused by low-pass filter in the sliding mode observer algorithm. In this method, firstly, the saturation function is proposed to replace the conventional sign function to reduce chattering, then the back electromotive force adaptive law is introduced to replace the low-pass filter so that the sliding mode observer obtains a better back electromotive force. Finally, the phase-locked-loop technique is used to extract more accurate rotor position information.

2. MATHEMATICAL MODEL OF PMA-SynRM

The structure of the permanent magnet-assisted synchronous reluctance motor and the schematic definition of the d and q axes are shown in Fig. 1.

In order to facilitate the analysis of the motor's characteristics, assumptions are made about the mathematical model in the ideal state of PMA-SynRM:

(1) Neglect motor core saturation and hysteresis loss;

(2) Only the fundamental wave is considered, and the higher harmonics are not considered;

(3) The three-phase windings are symmetrical to each other.

Equation (1) is the mathematical model expression for PMA-SynRM in a two-phase stationary coordinate system:

$$\begin{bmatrix} u_\alpha \\ u_\beta \end{bmatrix} = \begin{bmatrix} R_s + \frac{\mathrm{d}}{\mathrm{d}t} L_q & -\omega_e \left(L_d - L_q\right) \\ \omega_e \left(L_d - L_q\right) & R_s + \frac{\mathrm{d}}{\mathrm{d}t} L_q \end{bmatrix} \begin{bmatrix} i_\alpha \\ i_\beta \end{bmatrix} + \begin{bmatrix} E_\alpha \\ E_\beta \end{bmatrix} \tag{1}$$

where i_α, i_β and u_α, u_β are the stator current and stator voltage in the stationary coordinate system; R_s is the stator resistance; ω_e is the rotor angular velocity; L_d and L_q are the d, q inductances; E_α and E_β are the components of the extended back electromotive force in the α, β axes, and as shown in Eq. (2):

$$\begin{bmatrix} E_\alpha \\ E_\beta \end{bmatrix} = \left[\left(L_d - L_q\right) \left(\omega_e i_q + \frac{\mathrm{d}}{\mathrm{d}t} i_d \right) + \psi_f \omega_e \right] \begin{bmatrix} \cos\theta_e \\ \sin\theta_e \end{bmatrix} \tag{2}$$

where ψ_f is the magnetic chain generated by the permanent magnets of the motor rotor.

From Eq. (2), it is evident that the extended back electromotive force encompasses both the electric angular velocity and angle of the motor. Therefore, the utilization of a sliding mode observer enables the estimation of the back electromotive force, electric angular velocity, and angle position information of the motor.

3. DESIGN OF CONVENTIONAL SMO FOR PMA-SYNRM

3.1. Fundamentals of the Conventional SMO

The design of the sliding mode observer is based on the calculation of the error between the reference current and the feedback current of the motor. This error value is utilized to create a sliding mode surface, which is then used in conjunction with a high-frequency switching signal generated by the sign function. The purpose of this approach is to facilitate the rapid convergence of the estimated current of the motor to the actual current. By doing so, the back electromotive force of the motor can be obtained, enabling the estimation and calculation of the rotor position.

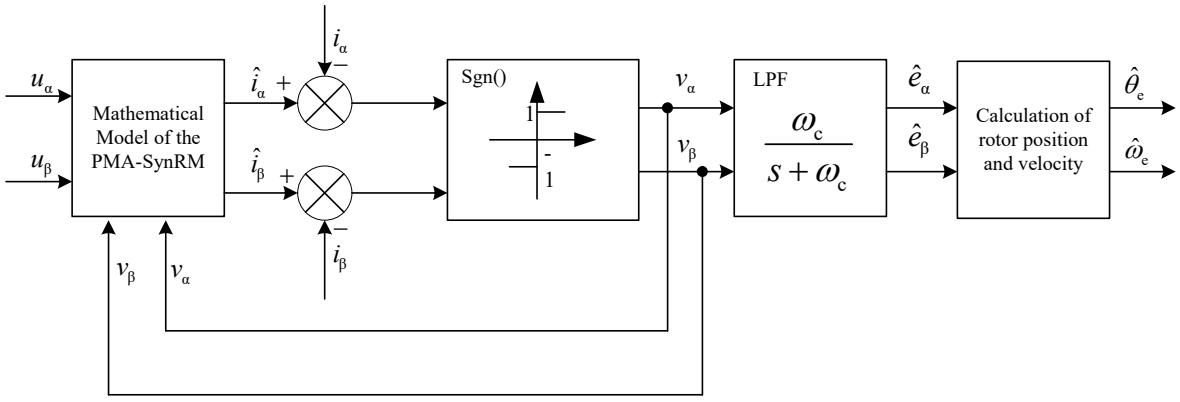

FIGURE 2. Block diagram of the conventional SMO.

The design of the conventional sliding mode observer uses the sign function to reconstruct the mathematical model of the motor Eq. (1) to obtain Eq. (3)

$$\frac{\mathrm{d}}{\mathrm{d}t}\begin{bmatrix} i_\alpha \\ i_\beta \end{bmatrix} = \frac{1}{L_\mathrm{q}}\begin{bmatrix} -R_\mathrm{s} & \omega_\mathrm{e}\left(L_\mathrm{d}-L_\mathrm{q}\right) \\ -\omega_\mathrm{e}\left(L_\mathrm{d}-L_\mathrm{q}\right) & -R_\mathrm{s} \end{bmatrix}\begin{bmatrix} i_\alpha \\ i_\beta \end{bmatrix} + \frac{1}{L_\mathrm{q}}\begin{bmatrix} u_\alpha \\ u_\beta \end{bmatrix} - \frac{1}{L_\mathrm{q}}\begin{bmatrix} E_\alpha \\ E_\beta \end{bmatrix} \tag{3}$$

Construct the conventional SMO as shown in Eq. (4):

$$\frac{\mathrm{d}}{\mathrm{d}t}\begin{bmatrix} \hat{i}_\alpha \\ \hat{i}_\beta \end{bmatrix} = \frac{1}{L_\mathrm{q}}\begin{bmatrix} -R_\mathrm{s} & \omega_\mathrm{e}\left(L_\mathrm{d}-L_\mathrm{q}\right) \\ -\omega_\mathrm{e}\left(L_\mathrm{d}-L_\mathrm{q}\right) & -R_\mathrm{s} \end{bmatrix}\begin{bmatrix} \hat{i}_\alpha \\ \hat{i}_\beta \end{bmatrix} + \frac{1}{L_\mathrm{q}}\begin{bmatrix} u_\alpha \\ u_\beta \end{bmatrix} - \frac{1}{L_\mathrm{q}}\begin{bmatrix} v_\alpha \\ v_\beta \end{bmatrix} \tag{4}$$

where $\hat{\omega}_e$ is the observed values of the motor's electrical angular velocity; $\hat{i}_\alpha$ and $\hat{i}_\beta$ are the observed values of the stator current; u_α and u_β are the observer inputs. In the conventional sliding mode observer, the sign function is chosen as the control convergence law; v_α and v_β are the estimated back electromotive force, respectively, whose expression is shown in Eq. (5).

$$\begin{bmatrix} v_\alpha \\ v_\beta \end{bmatrix} = \begin{bmatrix} h\mathrm{sgn}\left(\hat{i}_\alpha - i_\alpha\right) \\ h\mathrm{sgn}\left(\hat{i}_\beta - i_\beta\right) \end{bmatrix} \tag{5}$$

where h is the sliding mode gain coefficient. Define the stator current error as the sliding mode surface as shown in Eq. (6):

$$s_{\alpha,\beta} = \begin{bmatrix} \hat{i}_\alpha - i_\alpha \\ \hat{i}_\beta - i_\beta \end{bmatrix} \tag{6}$$

Making a difference between Eq. (3) and Eq. (4) gives Eq. (7) as:

$$\frac{\mathrm{d}}{\mathrm{d}t}\begin{bmatrix} \tilde{i}_\alpha \\ \tilde{i}_\beta \end{bmatrix} = \frac{1}{L_\mathrm{q}}\begin{bmatrix} -R_\mathrm{s} & \omega_\mathrm{e}\left(L_\mathrm{d}-L_\mathrm{q}\right) \\ -\omega_\mathrm{e}\left(L_\mathrm{d}-L_\mathrm{q}\right) & -R_\mathrm{s} \end{bmatrix}\begin{bmatrix} \tilde{i}_\alpha \\ \tilde{i}_\beta \end{bmatrix} + \frac{1}{L_\mathrm{q}}\begin{bmatrix} E_\alpha \\ E_\beta \end{bmatrix} - \frac{1}{L_\mathrm{q}}\begin{bmatrix} v_\alpha \\ v_\beta \end{bmatrix} \tag{7}$$

where $\tilde{i}_\alpha = \hat{i}_\alpha - i_\alpha$ and $\tilde{i}_\beta = \hat{i}_\beta - i_\beta$ are the stator current observation error. According to the sliding mode equivalent control theory, Eq. (8) can be obtained when the current error $\tilde{i}_\alpha = 0$, $\tilde{i}_\beta = 0$.

$$\begin{bmatrix} e_\alpha \\ e_\beta \end{bmatrix} = \begin{bmatrix} v_\alpha \\ v_\beta \end{bmatrix} = \begin{bmatrix} h\mathrm{sgn}\left(\hat{i}_\alpha - i_\alpha\right) \\ h\mathrm{sgn}\left(\hat{i}_\beta - i_\beta\right) \end{bmatrix} \tag{8}$$

where e_α and e_β are the back electromotive force obtained by the sliding mode observer.

The sign function in the conventional SMO leads to the presence of high harmonics in the signal, which needs to be filtered and processed by an LPF before position estimation, as shown in Eq. (9).

$$\begin{bmatrix} \hat{e}_\alpha \\ \hat{e}_\beta \end{bmatrix} = \frac{\omega_c}{s+\omega_c}\begin{bmatrix} v_\alpha \\ v_\beta \end{bmatrix} \tag{9}$$

Due to the presence of an LPF, a phase delay in the angle occurs, necessitating the need for angle compensation. The compensated rotor position and electrical angular velocity can be mathematically represented as Eq. (10)

$$\begin{cases} \hat{\theta}_\mathrm{eq} = \arctan(\frac{\hat{e}_\beta}{\hat{e}_\alpha}) \\ \hat{\theta}_e = \hat{\theta}_\mathrm{eq} + \arctan(\frac{\hat{\omega}_e}{\omega_c}) \\ \hat{\omega}_e = \int \hat{\theta}_e \mathrm{d}t \end{cases} \tag{10}$$

In conclusion, the block diagram illustrating the structure of position sensor-less vector control for a permanent magnet-assisted synchronous reluctance motor with a conventional sliding mode observer is depicted in Fig. 2.

3.2. Problem Analysis of SMO

From the principle of the sliding mode observer, it is evident that the sign function in the conventional sliding mode observer introduces a significant chattering effect on the system. Therefore, the implementation of a low-pass filter is necessary to

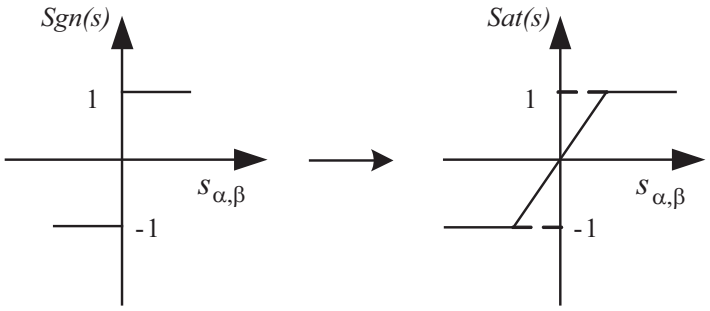

FIGURE 3. Schematic diagram of the sign and saturation function curve.

mitigate this effect during the filtering process. In the filtering process, the implementation of a low-pass filter is necessary to suppress high-frequency signals and decrease their amplitude. However, the introduction of this filter also results in a certain delay, causing a phase lag phenomenon between the high-frequency signals and the low-frequency signals. In this process, the frequency response of the low-pass filter can be considered as a decaying function, resulting in a greater suppression of the amplitude of high-frequency signals than low-frequency signals. As a consequence, high-frequency signals encounter increased latency as they traverse the filter, leading to a phase lag in the signal. The effectiveness of the low-pass filter in reducing chattering is limited and necessitates the incorporation of a phase compensation link. This addition increases the computational burden of the system and has the potential to decrease the accuracy of system estimation.

4. ADAPTIVE SMO DESIGN FOR PMA-SYNRM

4.1. Design of the Sliding Mode Function

In order to attenuate the chattering effect of the system and for ease of computation, the sign function in Eq. (5) is replaced with a saturation function as shown in Fig. 3.

In the control system based on saturated function with sliding mode observer, the stability of the control system is analyzed according to Lyapunov stability criterion, and Eq. (7) is further calculated to obtain Eq. (11).

$$\frac{\mathrm{d}}{\mathrm{d}t}\begin{bmatrix}\tilde{i}_\alpha\\ \tilde{i}_\beta\end{bmatrix} = \frac{1}{L_\mathrm{q}}\begin{bmatrix}-R_\mathrm{s} & \omega_\mathrm{e}\left(L_\mathrm{d}-L_\mathrm{q}\right)\\ -\omega_\mathrm{e}\left(L_\mathrm{d}-L_\mathrm{q}\right) & -R_\mathrm{s}\end{bmatrix}\begin{bmatrix}\tilde{i}_\alpha\\ \tilde{i}_\beta\end{bmatrix} + \frac{1}{L_\mathrm{q}}\begin{bmatrix}u_\alpha - v_\alpha\\ u_\beta - v_\beta\end{bmatrix} \tag{11}$$

Rewriting Eq. (11) into the form of Eq. (12), the

$$\dot{s} = As + B(e - hZ(s_{\alpha\beta})) \tag{12}$$

where $A = \begin{bmatrix} -\frac{R_s}{Lq} & \frac{\omega_e(L_d-L_q)}{Lq} \\ -\frac{\omega_e(L_d-L_q)}{L_q} & -\frac{R_s}{Lq} \end{bmatrix}$, $B = \begin{bmatrix} \frac{1}{L_q} \\ \frac{1}{L_q} \end{bmatrix}$, and the back electromotive force is $e = \begin{bmatrix} e_\alpha \\ e_\beta \end{bmatrix}$. According to the Lyapunov stability criterion, the Lyapunov function is shown in Eq. (13).

$$V(x) = \frac{(s_{\alpha\beta})^2}{2} \tag{13}$$

If the condition $\begin{cases} \dot{V}(x) = s_{\alpha\beta}\dot{s}_{\alpha\beta} < 0 \\ \lim_{x\to\infty} s_{\alpha\beta} = 0 \end{cases}$ is satisfied, then the system will gradually stabilize on the sliding mold surface.

$$\dot{V}(x) = As_{\alpha\beta}^T s_{\alpha\beta} + Bs_{\alpha\beta}^T(e - hZ(s_{\alpha\beta})) < 0 \tag{14}$$

When $Bs_{\alpha\beta}^T(e - hZ(s_{\alpha\beta})) < 0$ that satisfies $\dot{V}(x) < 0$, the range of sliding mode gain coefficients is derived:

$$h > \max(|e_\alpha|, |e_\beta|) \tag{15}$$

The system is stabilized when h satisfies Eq. (15).

4.2. Design of the Adaptive Law for Back Electromotive Force

In the saturated function SMO, it has been observed that the utilization of a low-pass filter still gives rise to the occurrence of angular phase delay. The cutoff frequency of the low-pass filter is dependent on the angular frequency of the real-time signal. Therefore, when the angular frequency of the motor, specifically the motor speed, varies, it becomes necessary to reselect the cutoff frequency and calculate the compensation angle. This results in an increase in the computational workload of the system. In this paper, the back electromotive force adaptive law is designed to effectively eliminate the high-frequency component while avoiding the problem of angle compensation.

Because the rate of change of motor angular velocity is much smaller than the rate of change of stator current, it can be set to $\frac{\mathrm{d}\omega_e}{\mathrm{d}t} = 0$, and the model of the back electromotive force of the permanent magnet-assisted synchronous reluctance motor can then be expressed as Eq. (16).

$$\begin{cases} \frac{\mathrm{d}e_\alpha}{\mathrm{d}t} = -\omega_e e_\beta \\ \frac{\mathrm{d}e_\beta}{\mathrm{d}t} = \omega_e e_\alpha \end{cases} \tag{16}$$

According to Eq. (16), the design of the back electromotive force adaptive law is as follows:

$$\begin{cases} \frac{\mathrm{d}\hat{e}_\alpha}{\mathrm{d}t} = -\omega_e\hat{e}_\beta - k(\hat{e}_\alpha - e_\alpha) \\ \frac{\mathrm{d}\hat{e}_\beta}{\mathrm{d}t} = \omega_e\hat{e}_\alpha - k(\hat{e}_\beta - e_\beta) \\ \frac{\mathrm{d}\hat{\omega}_e}{\mathrm{d}t} = \tilde{e}_\alpha\hat{e}_\beta - \tilde{e}_\beta\hat{e}_\alpha \end{cases} \tag{17}$$

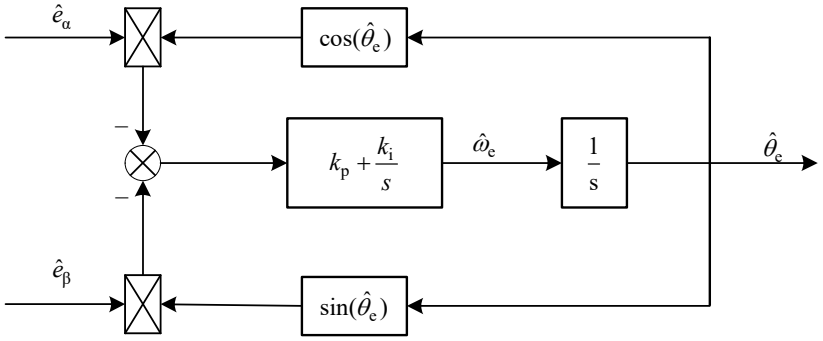

FIGURE 4. Phase-locked loop block diagram.

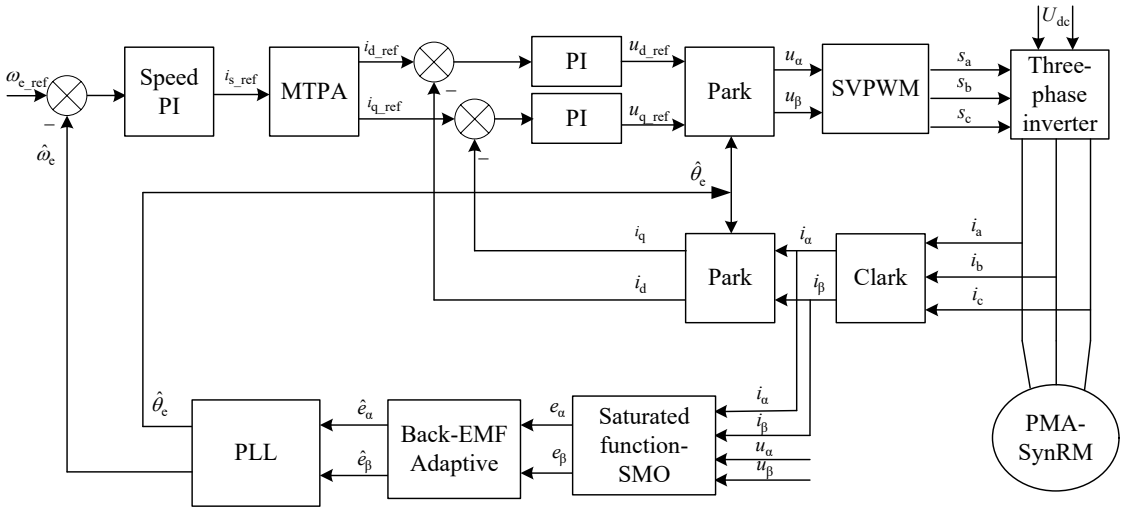

FIGURE 5. Block diagram of the improved control strategy.

where $\tilde{e}_\alpha = \hat{e}_\alpha - e_\alpha$, $\tilde{e}_\beta = \hat{e}_\beta - e_\beta$, k is an adjustable parameter, and Eq. (16) and Eq. (17) are differenced to obtain Eq. (18).

$$\begin{cases} \frac{\mathrm{d}\tilde{e}_\alpha}{\mathrm{d}t} = -\tilde{\omega}_e\hat{e}_\beta - k\tilde{e}_\alpha - \omega_e\tilde{e}_\beta \\ \frac{\mathrm{d}\tilde{e}_\beta}{\mathrm{d}t} = \tilde{\omega}_e\hat{e}_\alpha - k\tilde{e}_\beta + \omega_e\tilde{e}_\alpha \\ \frac{\mathrm{d}\tilde{\omega}_e}{\mathrm{d}t} = \tilde{e}_\alpha\hat{e}_\beta - \tilde{e}_\beta\hat{e}_\alpha \end{cases} \tag{18}$$

where the electrical angular velocity error $\tilde{\omega}_e = \hat{\omega}_e - \omega_e$.

The stability analysis of the designed adaptive back electromotive force is conducted based on the Lyapunov stability criterion, which characterizes the function as follows:

$$V = \frac{\tilde{e}_\alpha^2 + \tilde{e}_\beta^2 + \tilde{\omega}_e^2}{2} \tag{19}$$

To make $\dot{V} = -k(\tilde{e}_\alpha^2 + \tilde{e}_\beta^2) \leq 0$, $k > 0$ only need to satisfy

when $\dot{V} < 0$, so the adaptive back electromotive force adaptive law satisfies the Lyapunov criterion and has asymptotic stability.

4.3. Position Estimation

In SMO, the rotor position can be calculated using an inverse tangent function. In order to eliminate the effect of harmonics and high frequency chattering, the rotor position can be calculated by Phase-Locked Loop (PLL) technique with error feedback and cancellation capability, whose block diagram is shown in Fig. 4.

The input of the phase-locked loop is the motor's equivalent back electromotive force, which is extracted by the sliding mode observer. The phase-locked loop not only improves the electrical angular velocity of the rotor and the accuracy of position information, but also accurately tracks the actual operating state of the motor. When phase-locked loop technology is utilized to process the equivalent back electromotive force, the error signal of the back electromotive force is represented as Eq. (20).

$$\begin{aligned} \Delta e &= \hat{e}_\beta \cos\hat{\theta}_e - \hat{e}_\alpha \sin\hat{\theta}_e \\ &\approx \hat{e}_\beta \cos\hat{\theta}_e - \hat{e}_\alpha \sin\hat{\theta}_e \\ &\approx k\sin(\theta_e - \hat{\theta}_e) \end{aligned} \tag{20}$$

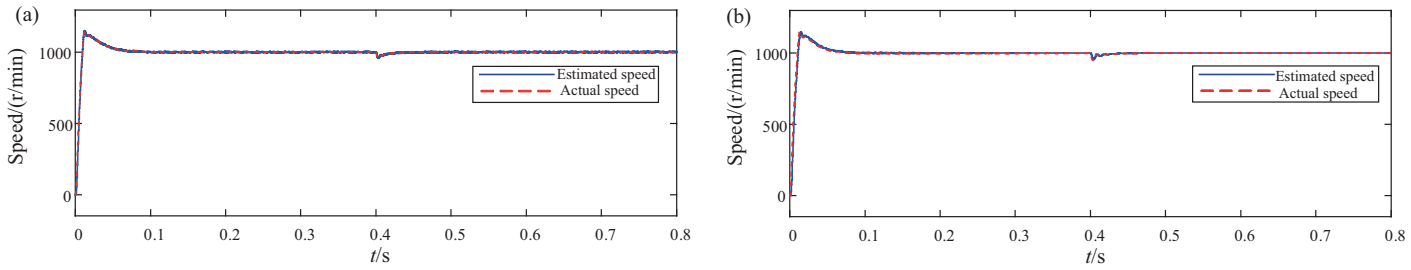

FIGURE 6. Comparison of simulation results of speed, (a) conventional, (b) improved.

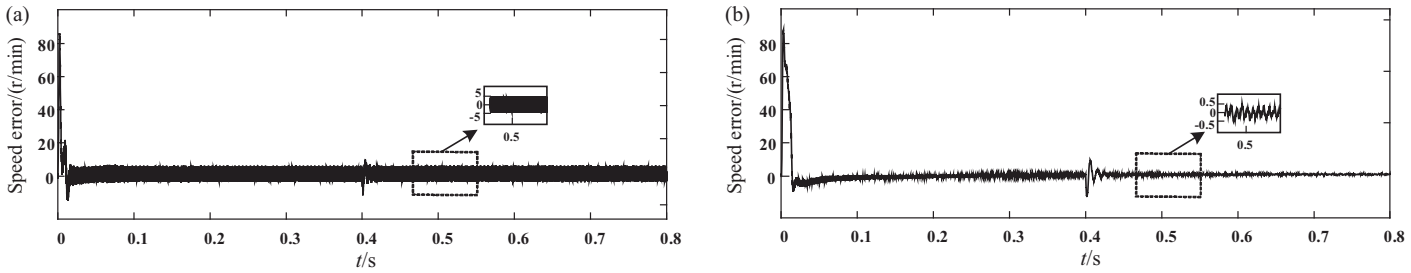

FIGURE 7. Comparison of simulation results speed error, (a) conventional, (b) improved.

TABLE 1. Parameters of PMA-SynRM.

Parameter/Unit	Value	Parameter/Unit	Value
Pole pairs	3	Rotor resistance/Ω	2.8
Rated power/kW	3	Inertia/J	0.002
Rated torque/N · m	9.5	Ld/mH	19.7
Rated speed/r/min	3000	Lq/mH	5.3
rated voltage/V	380	ψ_f/Wb	0.19

The rotor error $\theta_e - \hat{\theta}_e \leq \frac{\pi}{6}$, $\Delta e \approx k(\theta_e - \hat{\theta}_e) = k\Delta\theta_e$ is obtained as the transfer function to

$$G_{\text{PLL}} = \frac{\hat{\theta}_e}{\theta_e} = \frac{k_p s + k_i}{s^2 + k_p s + k_i} \tag{21}$$

where k_p and k_i are the proportional and integral gains of PLL. The error is mediated by the Proportional and Integral (PI) to obtain the rotor's electrical angular velocity, and the angular position information can be obtained by integrating the angle.

In summary, this paper presents the design of a saturation function and the back electromotive force adaptive law SMO for a control system of a permanent magnet assisted synchronous reluctance motor without a position sensor. The system is illustrated in Fig. 5.

5. SIMULATION RESULTS ANALYSIS

In order to verify the correctness and effectiveness of the proposed algorithm, this paper builds the ontology simulation of PMA-SynRM and its control model under the MATLAB/Simulink environment. It then proceeds to compare and analyze the conventional saturated-function SMO algorithm and the saturated-function adaptive SMO algorithm respectively. The motor parameters are shown in Table 1.

The simulation results of the PMA-SynRM position sensorless control system based on the conventional SMO with saturation function and the improved SMO combining the saturation function with the adaptive law of back electromotive force are shown in the following figures.

Figures 6 and 7 depict the performance comparison of the motor under sudden torque change conditions when it is controlled by the conventional saturated function SMO and improved SMO, respectively. The motor is given a reference speed of 1000 r/min, and the load torque mutates from 5 N · m to the rated torque of 9.5 N · m in 0.4 s. From Fig. 6, it is evident that the improved SMO estimation of the rotational speed exhibits a smoother profile and has less chattering effect than the conventional saturated function SMO. Fig. 7(a) demonstrates that the speed error of the conventional saturated function SMO stays within ±5 r/min after stabilization, and Fig. 7(b) demonstrates that the improved SMO can stabilize the speed error to within ±0.5 r/min. The improved SMO improves the speed accuracy of the whole control system by 90%, which proves that

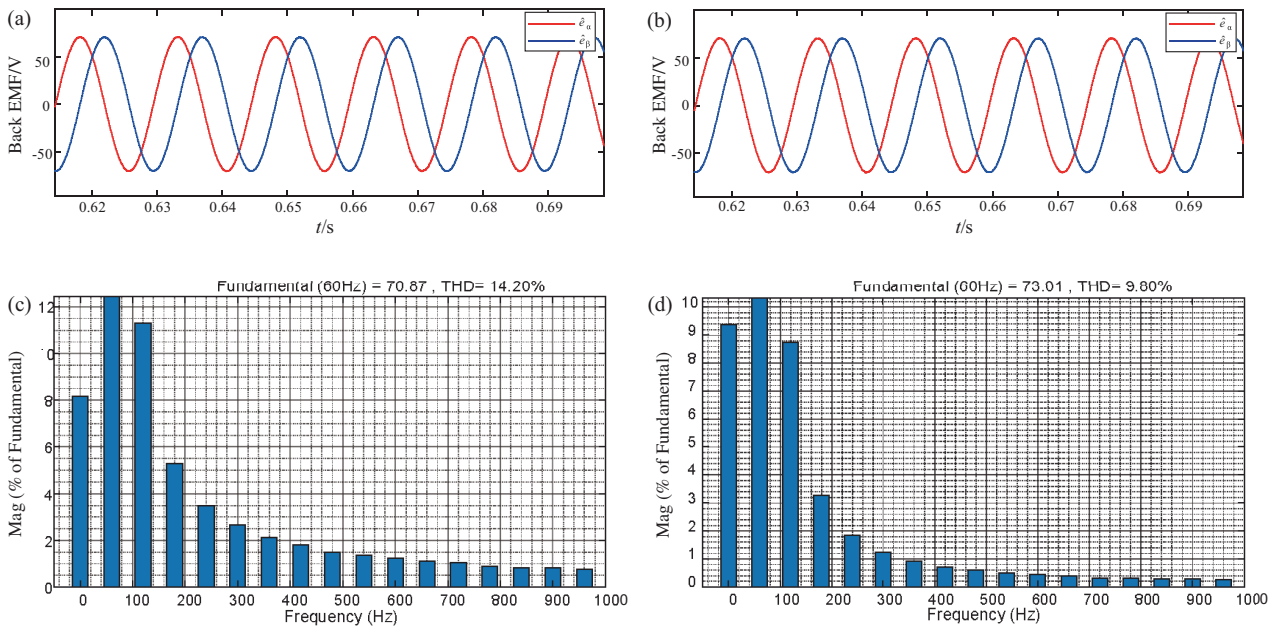

FIGURE 8. Comparison of simulation results for the back electromotive force.

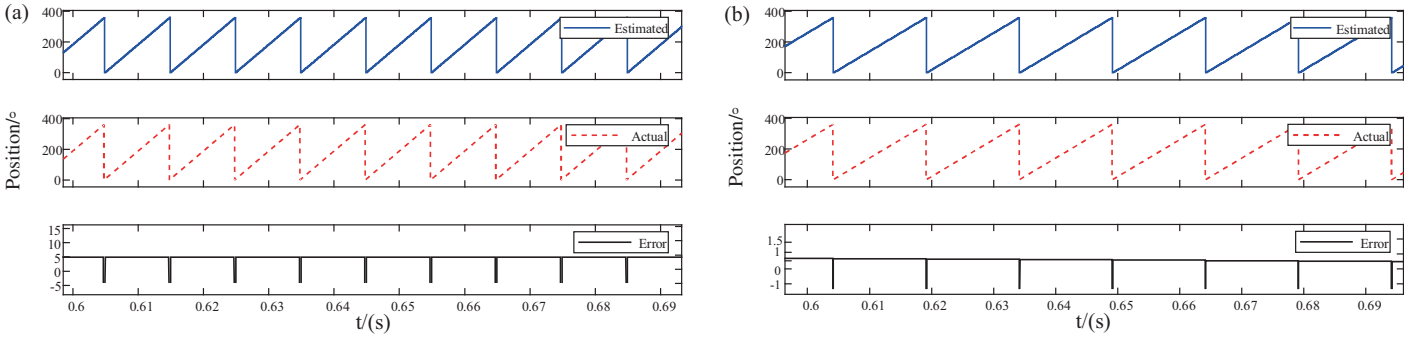

FIGURE 9. Comparison of simulation results for position, (a) conventional, (b) improved.

the improved SMO designed in this paper still maintains good dynamic performance after a sudden change of torque, and the estimated speed value is more accurate.

Figure 8 shows the comparison of the back electromotive force waveforms of the motor at the simulation condition of 1000 r/min reference speed and 5 N · m load torque. From Figs. 8(a) and (b), it can be observed that the observed back electromotive forces are close to sinusoidal waveforms. To further verify that there is less chattering and harmonics in the back electromotive force observed by the improved SMO, fast Fourier transform (FFT) harmonic analysis is performed when the speed tends to be stabilized. Fig. 8(c) represents the harmonic analysis of the conventional saturated function SMO, and the total harmonic component of the back electromotive force is THD = 14.20%. Fig. 8(d) shows the harmonic analysis of the improved SMO, and the total harmonic component of the back electromotive force is THD = 9.80%. The harmonic content is reduced by a total of 4.4%, providing evidence that the improved SMO demonstrates a decrease in harmonic content of the back electromotive force. This improvement effectively enhances the estimation accuracy of the system.

Figure 9 shows the position estimation tracking and error results when the motor is running stably at 1000 r/min, and the load torque is 5 N · m. The results are shown in Fig. 9(a). From the figure, it can be seen that the angle tracking effect is good, and the error between the estimated and actual angles of the rotor position in Fig. 9(a) is about 5°, while the error between the estimated and actual angles of the rotor position in Fig. 9(b) is about 0.7°. The simulation results show that the improved adaptive sliding mode observer control system makes the position estimation accuracy increase by 86%, which proves the feasibility and effectiveness of the adaptive sliding mode observer control system proposed in this paper.

6. CONCLUSION

In this paper, an adaptive SMO based on saturated function is proposed as a position sensorless control scheme for permanent magnet-assisted synchronous reluctance motor. Firstly, the conventional sign function is substituted with the saturation function, which effectively suppresses the chattering problem of the conventional SMO by utilizing its boundary layer

saturation property. Secondly, the introduction of the back electromotive force adaptive law, in conjunction with the replacement of the conventional low-pass filter, effectively improves the phase delay and phase compensation issues associated with the LPF. The stability conditions are determined by assessing its stability using the Lyapunov criterion. Finally, a more precise determination of the motor rotor position is achieved through the utilization of PLL technology. The simulation results demonstrate that the improved SMO, designed in this study, exhibits superior dynamic steady-state performance compared to the conventional SMO control system. The algorithm presented in this paper enhances the accuracy of speed estimation by 90% and position estimation by 86%, thereby establishing the feasibility and effectiveness of the proposed approach.

ACKNOWLEDGEMENT

This work Supported by the National Natural Science Foundation of China (51407021), the National Science Foundation of China under Grant (52377037).

REFERENCES

[1] Vagati, A., M. Pastorelli, G. Franceschini, and S. C. Petrache, "Design of low-torque-ripple synchronous reluctance motors," *IEEE Transactions on Industry Applications*, Vol. 34, No. 4, 758–765, 1998.

[2] Xu, M. M., G. J. Liu, Q. Chen, and W. X. Zhao, "Review on design and key technology development of permanent magnet assisted synchronous reluctance motor," *Proceedings of the CSEE*, Vol. 39, No. 23, 7033–7043, 2019.

[3] Wen, Z. K. and J. B. Chu, "Deadbeat direct torque control of PMASynRM based on stator field orientation," *Electric Machines & Control Application*, Vol. 49, No. 05, 20–26, 2022.

[4] Zheng, S. Y., X. Y. Zhu, L. Xu, *et al.*, "Design and performance analysis of pm-assisted synchronous reluctance motor considering high torque-quality ratio," *Chinese Journal of Electrical Engineering*, Vol. 42, No. 19, 7236–7248, 2022.

[5] Leuzzi, R., P. Cagnetta, S. Ferrari, P. Pescetto, G. Pellegrino, and F. Cupertino, "Transient overload characteristics of PM-assisted synchronous reluctance machines, including sensorless control feasibility," *IEEE Transactions on Industry Applications*, Vol. 55, No. 3, 2637–2648, 2019.

[6] Huang, H. and Y. S. Hu, *Design and Application of Permanent Magnet-assisted Synchronous Reluctance Motor*, Machinery Industry Press, 2017.

[7] Cao, H. P., M. M. Ai, and Y. B. Wang, "Research status and development trend of permanent magnet assisted synchronous reluctance motor," *Transactions of China Electrotechnical Society*, Vol. 37, No. 18, 4575–4592, 2022.

[8] Xie, Z. X., "Research on control strategies of permanent magnet-assisted synchronous reluctance motor," Ph.D. dissertation, Zhejiang University, Zhejiang, 2021.

[9] Niazi, P., H. A. Toliyat, and A. Goodarzi, "Robust maximum torque per ampere (MTPA) control of PM-assisted SynRM for traction applications," *IEEE Transactions on Vehicular Technology*, Vol. 56, No. 4, 1538–1545, 2007.

[10] Joo, K.-J., I.-G. Kim, J. Lee, and S.-C. Go, "Robust speed sensorless control to estimated error for PMa-SynRM," *IEEE Transactions on Magnetics*, Vol. 53, No. 6, 1–4, 2017.

[11] Wang, X. H., W. Z. Lian, M. Y. Zhai, *et al.*, "Sensorless control method of permanent magnet synchronous motor based on a modified sliding-mode observer," *Control Theory & Applications*, Vol. 40, 2023.

[12] Rahmatullah, R., A. Ak, and N. F. O. Serteller, "SMC controller design for DC motor speed control applications and performance comparison with FLC, PID and PI controllers," in *Intelligent Sustainable Systems*, Vol. 579, 607–617, 2023.

[13] Chakali, A. K., H. A. Toliyat, and H. Abu-Rub, "Observer-based sensorless speed control of PM-assisted SynRM for direct drive applications," in *2010 IEEE International Symposium on Industrial Electronics*, 3095–3100, Bari, Italy, 2010.

[14] Zhang, Z. and L. Zhou, "Sensorless control of a ferrite PM assisted-synchronous reluctance machines by using sliding mode observer and high frequency signal injection," *Elektronika Ir Elektrotechnika*, Vol. 22, No. 4, 11–15, 2016.

[15] Zhang, L. W., X. Li, and P. P. Song, "Sensorless vector control using a new sliding mode observer for permanent magnet synchronous motor speed control system," *Transactions of China Electrotechnical Society*, Vol. 34, No. S1, 70–78, 2019.

[16] Wu, C. L. and J. B. Chu, "Position sensorless control using an improved sliding mode observer of PMASynRM," *Electric Machines & Control Application*, Vol. 48, No. 07, 26–33, 2021.

[17] Zhao, F., W. Luo, F. Gao, *et al.*, "Sensorless hybrid control for permanent magnet synchronous motor using fuzzy sliding mode controller and two-stage filter observer," *Control Theory and Applications*, Vol. 37, No. 8, 1865–1872, 2020.